Biosynthesis and characterization of selenium nanoparticles using rind of watermelon (*Citrullus lanatus*)

Namrata Jha,[1] Sonia Johri,[1,*] Sadhana Shrivastava,[2] Poonam Gupta[1] and Kamini Yadav[2]

[1] *ITM University, Gwalior, M.P., India*
[2] *Jiwaji University, Gwalior, M.P., India*

Watermelon (*Citrullus lanatus*) is a cheap and easily available fruit in the local markets of India. The large edible fruit is a berry with a hard rind and no internal divisions, and is botanically called a pepo. The sweet, juicy flesh is usually deep red to pink, with many black seeds. The rind, which is the green skin that keeps all the waterlogged delicious fruit safe, is completely edible. The present study aimed to characterize and evaluate the presence of secondary metabolites in the rind. Therapeutic efficacy of watermelon rind against acrylamide toxicity in the lymphocyte cell line was also studied. As selenium is an important micronutrient, an attempt has been made to prepare selenium nanoparticles using the rind, followed by their characterization.

Keywords: DSC, FTIR, PSA, UV–visible

1. Introduction

Biosynthesis of nanomaterials (part of bionanotechnology) chiefly refers to the synthesis of metal nanoparticles using bioactive agents such as plant materials, microörganisms, and various kinds of biowaste including noncomestible parts of vegetables, fruit peel, eggshells and miscellaneous agricultural waste. Plants contain a varied range of secondary metabolites, including reducing (antioxidant) substances useful for the biosynthesis of nanoparticles. As plants are easily available with a stable supply they are good candidates for nanoparticle production, thereby extracting something beneficial from the plant (using different experimental methods).[1] Globally a high

* Corresponding author. E-mail: SoniaJohari@itmuniversity.ac.in

[1] Alagesan, V. & Venugopal, S. Green synthesis of selenium nanoparticles using leaves extract of *Withania somnifera* and its biological applications and photocatalytic activities. *BioNanoScience* **9** (2019) 105–116.

Nanotechnology Perceptions **18** (2022) 153–168
Received 15 September 2021; *accepted* 31 March 2022

doi: 10.4024/N12JH21A.ntp.18.02

intake of plant products is associated with reduced risk of succumbing to harmful diseases such as cancer. The widely encountered antioxidant molecules—e.g., found in chocolate with high cocoa content—are also beneficial for disease prevention.[2] These molecules also suggest synthetic applications where ultramild reducing conditions are required; bionanotechnology is an eco-friendly and nontoxic perspective for valorizing biomaterials (Fig. 1).[3]

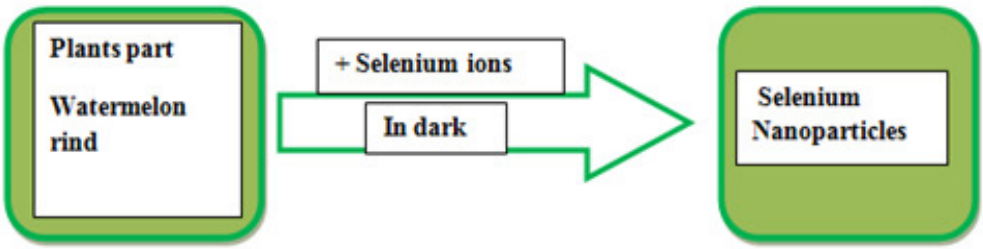

Figure 1. Flow chart of the formation of selenium nanoparticles.

1.1 Watermelon

Watermelon (*Citrullus lanatus*) is a widely acceptable, edible fruit. The red interior part is sweet and edible but the green outer part is usually discarded and considered as waste.[4] Watermelons are reported to be rich in carotenoids like lycopene, phytofluene, phytoene, β-carotene and lutein. They consist of different types of protein, rich in functional group such as hydroxyl and carboxyl, and components such as pectin, citrulline and cellulose.[4,5] On average, watermelon consists of 68% pulp, 30% rind and the rest seeds, which are typically discarded but can be used for cattle feed, and as vegetables in some parts of the country. The rind of the fruit is prescribed in cases of alcohol poisoning and diabetes.[6] Watermelon is used in northern Sudan to treat burns, swellings, rheumatism and gout, and as a laxative.[7] Studies have revealed the presence of a variety of phytochemicals in the rind, having great biological significance. Watermelon rind has also been used as a biosorbent for the removal of dyes and heavy metals from solution.[8]

---

[2] Szerlauth, A., Murath, S., Viski, S. & Szilagyi, I. Radical scavenging activity of plant extracts from improved processing. *Heliyon* **5** (2019) E02763.

[3] Yazhiniprabha, M. & Vaseeharan, B. In vitro and in vivo toxicity assessment of selenium nanoparticles with significant larvicidal and bacteriostatic properties. *Mater. Sci. Engng C* **103** (2019) 109763.

[4] Lakshmipathy, R. et al. Watermelon rind-mediated green synthesis of noble palladium nanoparticles: catalytic application. *Appl. Nanosci.* **5** 015) 223–128.

[5] Patra, J.K. & Baek, K.H. Novel green synthesis of gold nanoparticles using *Citrulluslanatus* rind and investigation of proteasome inhibitory activity, antibacterial and antioxidant potential. *Intl J. Nanomed.* **10** (2015) 7253–7264.

[6] Duke, J.A. & Ayensu, E.S. *Medicinal Plants of China*. Algonac: Reference Publications (1985).

[7] Schippers, R.R. *African Indigenous Vegetables: An overview of the cultivated species*. Chatham: Natural Resources Institute/ACP-EU Technical Centre for Agricultural & Rural Cooperation (2000).

[8] Huang, M., Jiao, J., Wang, J., Xia, Z. & Zhang, Y. Exposure to acrylamide induces cardiac developmental toxicity in zebrafish during cardiogenesis. *Environ. Pollution* **234** (2018) 656–666.

1.2 Acrylamide

According to the World Health Organization (WHO), more than 100,000 different chemical compounds are discharged into the environment every year from different industries. Hence it is not surprising that contaminating (i.e., unnatural) chemicals, such as polycyclic aromatic hydrocarbons, aromatic amines, amino dyes and alkenes (some of which may cause cancer) are found in foods and food products;[9] there is a high production of chemicals having adverse effects on other products that are themselves made by industry (e.g., processed foods).[10]

One of these chemicals is acrylamide. Exposure to may lead to different neurotoxic effects in humans and in experimental animals. Acrylamide has been recognized as mutagenic, carcinogenic, neurotoxic and an endocrine disruptor both in humans and experimental animals. The neurotoxic effects of acrylamide exposure in humans include ataxia, skeletal muscle weakness, numbness of the extremities, and other symptoms related to polyneuropathy.[11] Acrylamide has a low molecular weight, is composed of carbon, hydrogen, nitrogen and oxygen atoms and can be dissolved in water.[12] It is used in various industries, in the form of polyacrylamide utilized as flocculent for waste water treatment, as adhesives, soil stabilizers and in laboratory gels.[13] Acrylamide is considered as both an environmental and occupational pollutant. It can be formed during the Millard reaction, especially in food products containing asparagine and glucose that are processed and cooked. Its residues have been found in processed foods such as bread from various types of cereals and those derived from potatoes.[14]

1.3 Selenium nanoparticles

Plant-synthesized nanoparticles are much better than others in terms of synthesis, safety, simplicity and ecological considerations.[15] The biosynthesis of NPs is preferred over their "green" synthesis. Interest in nanoparticles (NPs) has evolved due to their novel possibilities in drug discovery and transport and other fields such phytochemistry, electronics, energy production, etc.[16]

---

[9] Kopanska, M., Muchacka, R., Czecha, J., Batoryna, M. & Formicki, G. Acrylamide toxicity and cholinergic nervous system. *J. Physiol. Pharmacol.* **60** (2018) 847–858.

[10] Kianfar, M., Nezami, A., Mehri, S., Hosseinzadeh, H., Hayes, A.W. & Karimi, G. The protective effect of fasudil against acrylamide induced cytotoxicity in PC 12 cells. *Drug Chem. Toxicol.* **43** (2018) 595–601.

[11] Raldua, D., Casado, M., Prats, E., Faria, M., Castellvi, P.F., Perez, Y., Alfonso, I., Hsu, Y.C., Arick II, A.M., Reyero, G.N., Ziv, T., Lulu, B.S., Admon, A. & Pina, B. Targeting redox metabolism: The perfect storm induced by acrylamide poisoning in the brain. *Sci. Rep.* **10** (2020) 312.

[12] Kumar, J., Das, S. & Teoh, S.L. Dietary acrylamide and the risks of developing cancer: Facts to ponder. *Frontiers Nutr.* **5** (2018) 14.

[13] Zamani, E., Shokrzadeh, M., Ziar, A., Abedian-Kenari, S. & Shaki, F. Acrylamide attenuated immune tissues' function via induction of apoptosis and oxidative stress: Protection by L-carnitine. *Human Exp. Toxicol.* **37** (2018) 859–869.

[14] Liu, Y., Wang, P., Chen, F., Yuan, Y., Zhu, Y., Yan, H. & Hu, X. Role of plant polyphenols in acrylamide formation and elimination. *Food Chem.* **186** (2015) 46–53.

[15] Patra, J.K., Das, G. & Baek, K.H. Phyto-mediated biosynthesis of silver nanoparticles using the rind extract of watermelon (*Citrulluslanatus*) under photo-catalyzed condition and investigation of its antibacterial, anticandidal and antioxidant efficacy, *J. Photochem. Photobiol B* **161** (2016) 200–210.

[16] Khurana, A., Tekula, S., Saifi, M.A., Venkatesh, P. & Godugu, C. Therapeutic applications of selenium nanoparticles. *Biomed. Pharmacotherapy* **111** (2019) 802–812.

A nanoparticle can increase the therapeutic efficacy of ionized drugs, enabling them to penetrate inside cells and target other biological components like proteins, oligopeptides, DNA and RNA.[17]

Se NPs have potent free radical-scavenging effects, in both *in vitro* as well as *in vivo*, and can protect DNA from oxidative damage.[18] Se is an important element in selenoenzymes, notably glutathione peroxidase, which helps in the prevention of free radical damage to cells and tissues *in vivo*.[14,19] Selenium is a trace element essential for the maintenance of human health; approximately 5.1 μmol/day is supposed to be the upper intake limit required for an adult human being.[20] Se NPs possess anticarcinogenic activity against several types of cancers.[21] Also, Se NPs show unique antimicrobial activity against *Candida albicans,*[22] *Proteus mirabilis and Pseudomonas aeruginosa.*[23] Accordingly, Se NPs could be highly recommended for use in biomedical and nutritional applications. Low selenium intake can contribute to morbidity and mortality, caused by infectious as well as chronic diseases.[24,25] The recommended dietary allowance (RDA) for selenium amounts to 0.7 μmol per day for both men and women.[26]

The present study aims to elucidate the therapeutic potential of selenium nanoparticles in watermelon rind, and its secondary metabolite composition.

2. Materials and methods

2.1 Rind extract preparation

Fresh watermelons were purchased from a local vendor. The rinds were separated, washed thoroughly and chopped into pieces and shade-dried for few days, weighed and kept in an oven

---

[17] Sharma, G., Sharma, A.R., Bhavesh, R., Park, J., Ganbold, B., Nam, J.S. & Lee, S.S. Biomolecule-mediated synthesis of selenium nanoparticles using dried Vitisvinifera (raisin) extract. *Molecules* **19** (2014) 2761–2770.

[18] Batten, C.A. et al. A real time RT-PCR assay for the specific detection of Peste des petits ruminants virus. *J. Virol. Methods* **171** (2011) 401–404.

[19] Zhang, W., Chen, Z., Liu, H., Zhang, L., Gao, P. & Li, D. Biosynthesis and structural characteristics of selenium nanoparticles by *Pseudomonas alcaliphila*. *Colloids Surf. B* **88** (2011) 196–201.

[20] Rayman P.M. Selenium in cancer prevention: a review of the evidence and mechanism of action. *Proc. Nutr. Soc.* **64** (2005) 527–542.

[21] Huang, J.K., Ma, P.L., Ji, S.Y., Zhao, X.L., Tan, J.X., Sun, X.J., Huang, F.D. Age-dependent alterations in the presynaptic active zone in a Drosophila model of Alzheimer's Disease. *Neurobiol. Disease* **51** (2013) 161–167.

[22] Kheradmand, E., Rafii, F., Yazdi, H.M., Sepahi, A.A., Shahverdi, R.A. & Oveisi, R.M. The antimicrobial effects of selenium nanoparticle-enriched probiotics and their fermented broth against *Candida albicans*. *J. Pharm. Sci.* **22** (2014) 22–48.

[23] Shakibaie, M., Forootanfar, H., Golkari, Y., Khorsand, M.T. & Shakibaie, R.M. Anti- biofilm activity of biogenic selenium nanoparticles and selenium dioxide against clinical isolates of *Staphylococcus aureus, Pseudomonas aeruginosa,* and *Proteus mirabilis*. *J. Trace Element Med. Biol.* **29** (2015) 235–241.

[24] Navarro-Alarcon, M. & Cabrera-Vique, C. Selenium in food and the human body: a review. *Sci. Total Environ.* **400** (2008) 115–141.

[25] Gunti, L., Dass, R.S. & Kalagatur, N.K. Phytofabrication of selenium nanoparticles from *Emblica officinalis* fruit extract and exploring its biopotential applications: Antioxidant, antimicrobial, and biocompatibility. *Frontiers Microbiol.* **10** (2019) 931.

[26] Yamasaki, K., Hashimoto, A., Kokusenya, Y., Miyamoto, T. & Sato, T. Electrochemical method for estimating the antioxidative effects of methanol extracts of crude drugs. *Chem. Pharm. Bull.* **42** (1994) 1663–1665.

at 85 °C for 48 h. The fine powder obtained after comminution was sieved and stored in a desiccator for further use.[25]

2.2 Aqueous rind extract preparation (decoction)

1 g of fine watermelon rind powder was extracted by boiling with distilled water (1:20 w/w) for 4–6 h, then filtered; extraction was repeated until the extract was colorless. The filtrate was concentrated for further analysis by evaporation in a water bath.[26]

2.3 Biosynthesis of selenium nanoparticles

2 mL of aqueous extract was added to 10 mL of 10 mM sodium selenite solution while mixing with a magnetic stirrer bar. Then the solution was placed in the dark at 27 ± 2 °C in an orbital shaker for 24 h or until a colour change was observed, due to reduction of the selenite.[25]

2.4 Phytochemical screening of watermelon rind extract

Qualitative phytochemical analysis of the crude powder was carried out as follows:

Tannins (ferric chloride test): 1 mg of rind extract was diluted in 1 mL of distilled water followed by addition of 1 mL of 5% ferric chloride solution. A dark green colour indicates the presence of tannins, and a blue or bluish-black colour indicates the presence of phenols.

Alkaloids (Mayer's test): 1 mg of rind extract was dissolved in few drops of acetic acid followed by Mayer's reagent. No white precipitate indicates the absence of alkaloids.

Carbohydrates (Fehling's test): 1 mg of rind extract was added to 1 mL of ethanol followed by 1 mL of Fehling's solution A:B (1:1). Formation of a red precipitate indicates the presence of carbohydrate.

Steroids (Liebermann–Burchard reaction): 20 mg of rind extract was dissolved in 1 mL chloroform, 1 mL acetic acid and 1 mL acetic anhydride. The solution was heated for 2–3 minutes, which results in conversion of the pink colour to green if steroids are present.

Saponins (foam test): 1 mg of rind extract was diluted in 7–8 mL distilled water. Frothing persistence indicates the presence of saponins.

Coumarins (sodium hydroxide test): 2–4 mg of rind extract was placed in a test tube and 1 mL ethanol followed by 1 mL of 2 N sodium hydroxide solution added; dark fluorescence indicates the presence of coumarins.

Carboxylic acid (effervescence test): 20 mg of rind extract was diluted in 1 mL distilled water in a test tube followed by addition of 1 mL 1 N sodium bicarbonate solution. Brisk effervescence indicates the presence of carboxylic acid.

Resin (acetone test): 20 mg of rind extract was diluted in 1 mL distilled water and 1 mL acetone added; turbidity indicates the presence of resin.

Quinone (sulfuric acid test): 20 mg of rind extract was taken in a test tube to which 1 mL ethanol and 1 mL 2 N sulfuric acid were added; a pink-purple-red colour indicates the presence of quinone.[27]

---

[27] Parekh, J. & Chanda, V.S. *In vitro* antimicrobial activity and phytochemical analysis of some Indian medicinal plants. *Turkish J. Biol.* **31** (2007) 53–58.

2.5 Characterization

2.5.1 UV–vis spectroscopy

Se NPs were characterized in a PerkinElmer UV–vis spectrophotometer: scan 200–1000 nm at 480 nm/min. Data was recorded and analysed by UV Winlab software.

2.5.2 Fourier transform infrared (FTIR) spectroscopy

An FTIR spectrophotometer (Perkin Elmer – Spectrum FT-IR with DTGS detector) was used to determine different the functional groups present in the Se NPs. The rind extract was dried and ground with a pestle and mortar and the spectrum recorded in the range 4000–400 cm^{-1}.

2.5.3 X-ray diffraction (XRD)

XRD is one of the most extensively used techniques for the characterization of NPs; it helps in detecting the crystalline or amorphous nature of the sample by precise quantification of peak broadening.[28] The Se NPs were examined in a Rigaku Miniflex 600 instrument, using D/tex Ultra software. Slit width was 10.00 mm and the θ–2θ range was 2000–9000°.

2.5.4 Transmission electron microscopy (TEM)

TEM is widely used to observe the size of small NPs through imaging, and reveals crystalline phase/crystallographic orientation through electron diffraction patterns, and the chemical composition by means of the characteristic spectrum of emitted X-rays. Samples were prepared by placing a drop of the Se NP suspension on carbon-coated copper grids and allowing the water to evaporate. Micrographs were recorded with Gatan Microscopy Software.[29,30]

2.5.5 PSA (particle size snalyser)

Particle sizes in suspension were determined with a laser diffraction particle size analyser (Shimadzu SALD-2300). The refractive index of the medium (water) was taken to be 1.33.[31]

2.5.6 Differential scanning calorimetry (DSC)

Thermal analysis was conducted with a Shimadzu TGA-50 thermogravimetric analyser from 15 to 300 °C.[32]

---

[28] Rehani, B.R., Joshi, P.B., Lad, K.N. & Pratap, A. Crystallite size estimation of elemental and composite silver nano-powders using XRD principles. *Indian J. Pure Appl. Phys.* **44** (2006) 157–161.

[29] Jiang, H.B.L.Y., Wong, C.C., Cheng, K.W. & Chen, F. Evaluation of two methods of antioxidants from medicinal plants, *Analyt. Bioanalyt. Chem.* **388** (2007) 483–488.

[30] Bosquillon, C., Lombry, C., Preat, V. & Vanbever, R. Comparison of particle sizing techniques in the case of inhalation dry powders. *J. Pharm. Sci.* **90** (2001) 2032-2041.

[31] Srivastava, N. & Mukhopadhyay, M. Biosynthesis and structural characterization of selenium nanoparticles using *Gliocladium roseum*. *J. Cluster Sci.* **26** (2015) 1473–1482.

[32] Chu, Q., Chen, W., Jia, R., Ye, X., Li, Y., Liu, Y., Jiang, Y. & Zheng, X. *Tetrastigma hemsleyanum* leaves extract against acrylamide-induced toxicity in HepG2 cells and *Caenorhabditis elegans*. *J. Hazardous Mater.* **393** (2020) 122364.

2.6 *In vitro* study

2.6.1 Chemicals and biochemicals

Acrylamide and Roswell Park Memorial Institute medium (RPMI 1640) were procured from Sigma–Aldrich. Water was triply distilled. Ficoll-Paque, fetal bovine serum (FBS), streptomycin, gentamycin, penicillin G, trypan blue dye, MTT assay reagents (EDTA, $NaHCO_3$, KCl, NaCl, KH_2PO_4, acetic acid and TCA) were of analytical grade obtained from Merck and tris base was obtained from Sigma–Aldrich.

2.6.2 Dose preparation

A suspension of 5 mM acrylamide was prepared in triply distilled water.

2.6.3 Dose optimization

Watermelon rind extract (15 mg) was dissolved in RPMI medium and the volume was made up to 3 mL. Different amounts were administered to 96-well plates to select the optimum dose; lymphocytes were treated with the aqueous rind extract at 6 different concentrations 25–500 μg/mL after acrylamide exposure.

2.6.4 In vitro medium

0.82 g RPMI, 100 mg $NaHCO_3$, 20 mg streptomycin, 37.5 μL gentamycin and 6 mg penicillin G were dissolved in 20 mL autoclaved triply distilled water and 10 mL FBS added to it.

2.6.5 Isolation of lymphocytes

A blood sample was derived from a healthy female rat and collected with the help of a capillary in a test tube with one pinch of EDTA, diluting in 2 mL phosphate buffer saline (PBS) at pH 7.4. The layer formed upon adding 4 mL Ficoll-Paque was centrifuged for 10 min at 2000 rpm. The white buffy layer containing lymphocytes was separated and transferred to a new tube. The collected lymphocyte layer was diluted with PBS pH 7.5 in the ratio of 1:1 and centrifuged at 2000 rpm for 10 min after which the pellet was collected. After washing the cells with RPMI 1640 (containing 10% FBS) twice, cells were cultured in RPMI 1640 (containing 10% FBS) with 1% antibiotic in the flask and incubated in a CO_2 incubator (5% CO_2, 90% humidity) at 37 °C.[33]

2.6.6 Maintenance

Lymphocytes cell were inoculated and grown in tissue culture flasks at 37 °C in the CO_2 incubator. Medium was changed when the colour changed. Fresh medium was placed in culture flasks under sterile conditions. Passaging was done at the subconfluent stage of cells, depending on the mass-doubling time.

---

[33] Ngema, S.S., Basson, A.K. & Maliehe, T.S. Synthesis, characterization and application of polyacrylamide grafted bioflocculant. *Phys. Chem. Earth* **115** (2020) 102821.

2.6.7 Subculturing

Medium of the flasks with subconfluent growth was changed followed by centrifugation at 2000 rpm for 10 min. The pellet was collected and washed with PBS. The tube was centrifuged at 2000 rpm for 10 min and the supernatant was discarded. Cells were resuspended in complete growth medium and were counted and checked for viability with trypan blue. After achieving 70–80% confluence, the next subculturing was performed.[34]

2.6.8 Cell viability assay

Cell viability means the proportion of healthy cells in a sample, calculated as

$$\%\ cell\ growth = \frac{cell\ growth\ in\ the\ presence\ of\ test\ material}{cell\ growth\ in\ the\ absence\ of\ test\ material}$$

and 0% growth inhibition ≡ 100% cell growth.

3. Results and discussion

3.1 Biogenic synthesis and characterization of Se NPs

Rind extraction efficiency achieved by using boiling water was greater than that achieved with other methods, e.g. using 80% methanol or other alcohols.[35,36]

Initially, the sodium selenite solution was colourless; it turned brick-red after the addition of rind extract and incubation for 24 h (Fig. 2). The colour is due to the excitation of surface plasmons and indicates reduction of sodium selenite into elemental selenium by the action of phenolics, flavonoids and tannins in the rind, further confirmed by UV–vis spectrophotometry.[25]

Figure 2. Synthesis medium: (left) shortly after the start of incubation; (right) after 24 h incubation.

[34] Pascua-Maestro, R., González, E., Lillo, C., Ganfornina, M.D., Falcón-Pérez, J.M. & Sanchez, D. Extracellular vesicles secreted by astroglial cells transport apolipoprotein D to neurons and mediate neuronal survival upon oxidative stress. *Frontiers Cell Neurosci.* **12** (2019) 526.

[35] Li, H.B., Jiang, Y., Wong, C.C., Cheng, K.W. & Chen, F. Evaluation of two methods for the extraction of antioxidants from medicinal plants. *Analyt. Bioanalyt. Chem.* **388** (2007) 483–488.

[36] Srivastava, N. & Mukhopadhyay, M. Biosynthesis and structural characterization of selenium nanoparticles mediated by Zooglearamigera. *Powder Technol.* **244** (2013) 26–29.

3.2 Phytochemical screening of aqueous rind extract

Carbohydrates, steroids, saponins, tannins, coumarins and carboxylic acids were present in significant amounts whereas phenol was relatively less and no alkaloid was detected (Table 1).

Table 1.Phytochemicals in aqueous extract of watermelon rind.

Test	Function	Result
Mayer's	Alkaloids	Negative
Fehling	Carbohydrate	Positive
Liebermann	Steroids	Positive
Saponins	Foam	Positive
Ferric chloride	Tannin	Positive
Ferric chloride	Phenol	Smaller amount
Sodium hydroxide	Coumarins	Positive
Effervescence	Carboxylic	Positive
Acetone	Resin	Positive
Sulfuric acid	Quinone	Positive

3.3 UV–vis spectroscopy

Rind extract alone is rather opaque below 400 nm (Fig. 3). During incubation, a distinct peak appears at about 210 nm (Fig. 4), indicating the formation of selenium nanoparticles.[25]

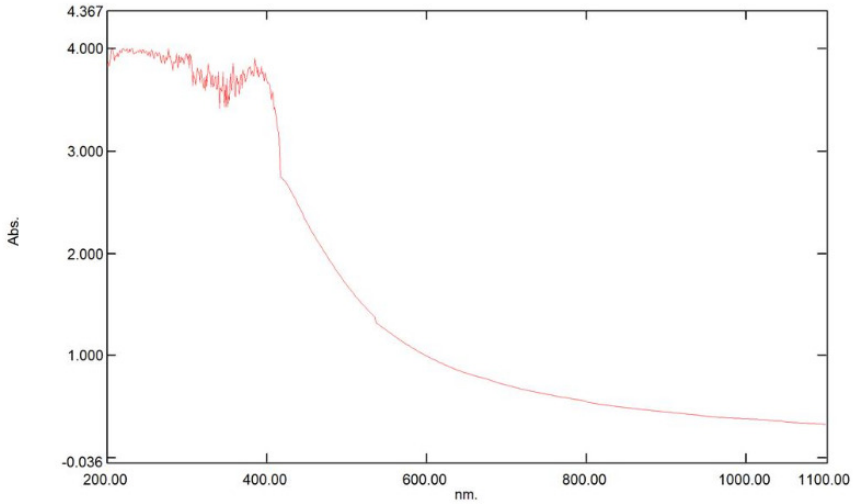

Figure 3.UV–vis absorption spectrum of the aqueous extract of watermelon rind.

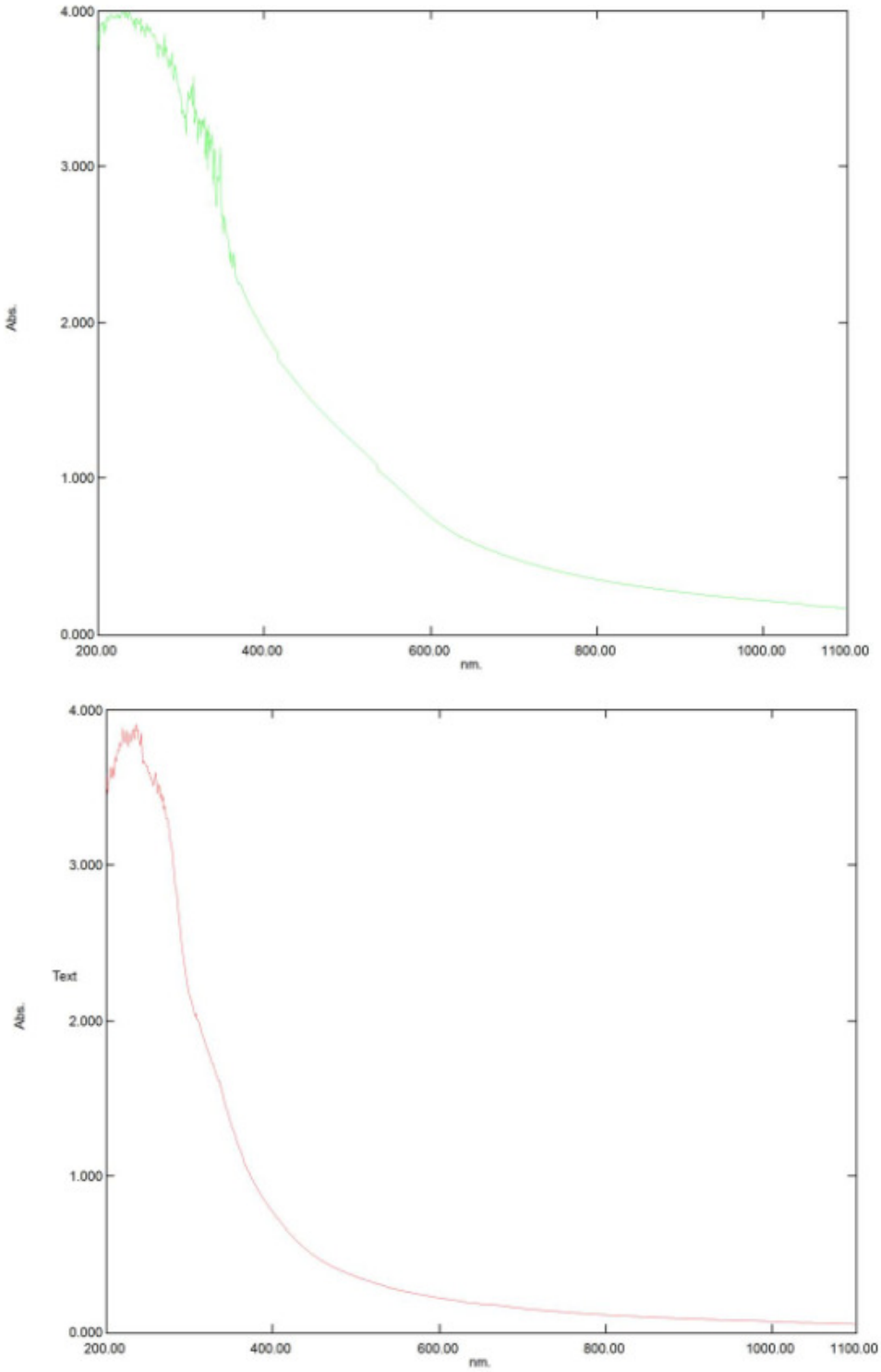

Figure 4. UV–vis absorption spectra (top) before incubation; (bottom) after incubation.

3.4 FTIR spectroscopy

Aqueous extract of watermelon rind absorption bands are given in Table 2 with assignments (cf. Fig. 5), indicating the presence of secondary metabolites responsible for reduction of the selenium ions and the formation of SeNPs through a reduction and capping process. [31,37] The spectrum of the Se NPs is shown in Fig. 6 with assignments given in Table 3.

Table 2. Functional groups detected in aqueous extract watermelon rind.

S. No.	Peak/cm^{-1}	Group	Compound	Appearance
1.	3340.03	O–H stretch	Alcohol	Strong
2.	1634.72	C=C stretch	Alkene	Medium

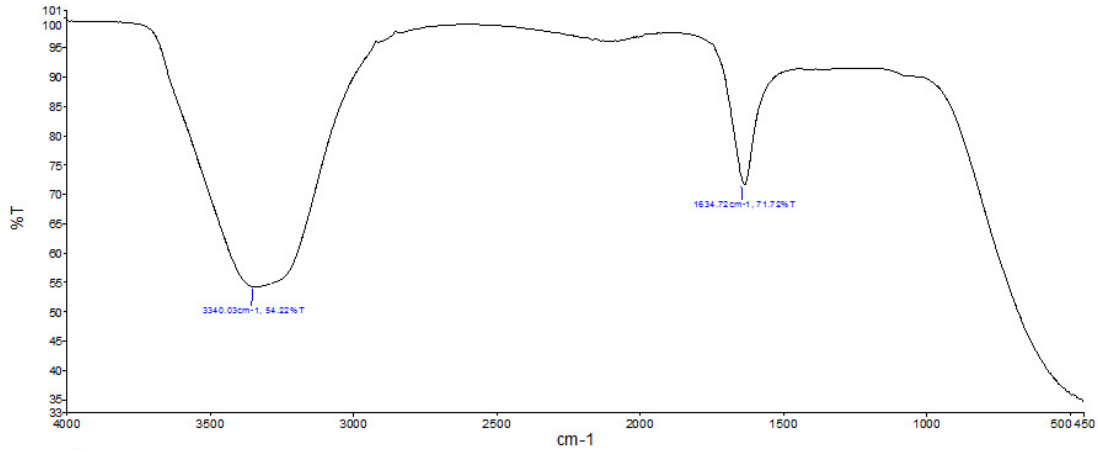

Figure 5. Fourier transform infrared spectrum of aqueous extract of watermelon rind.

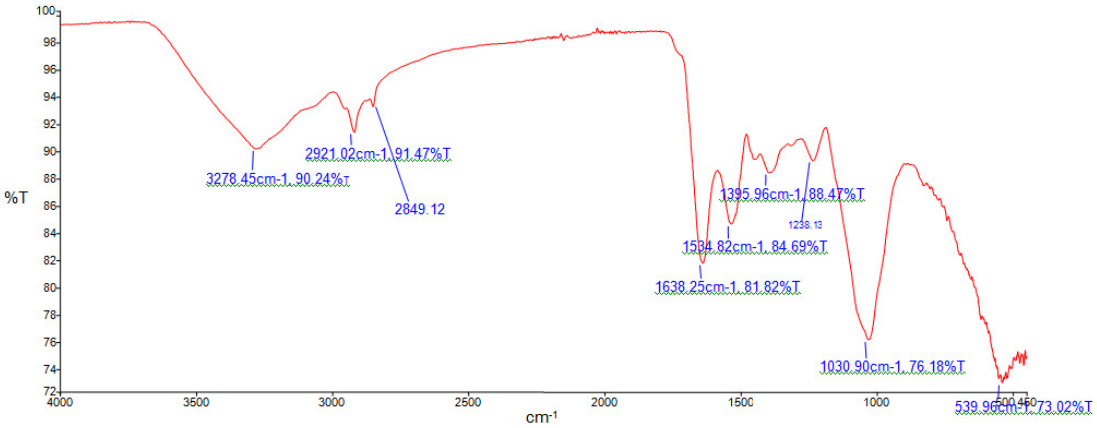

Figure 6. Fourier transform infrared spectrum of selenium nanoparticles synthesized from watermelon rind extract.

[37] Kazemi, M. et al. Evaluation of antifungal and photocatalytic activities of gelatin-stabilized selenium oxide nanoparticles. *J. Inorg. Organomet. Polym.* **30** (2020) 3036–3044.

Table 3.Functional groups of selenium nanoparticles extracted from watermelon rind extract.

Peak No	Peak/cm^{-1}	Group	Compound	Appearance
1	3278.45	O–H stretching	Alcohol	Strong
2	2921	C–H stretching	Methylene asymmetric	Strong
3	2849	O–CH_3stretching	Methoxy	Medium
4	1638	C=C stretching	Alkene	Strong
5	1535	>N–H stretching	Secondary amine	Medium
6	1395	O–H stretching	Tertiary alcohol	Medium
7	1238	C–O stretching	Alkyl aryl ether	Weak
8	1030	C–C stretching		Strong
9	539	OH stretching	Phenolic	Strong

3.5 XRD

The XRD pattern of the Se NPs can be seen in Fig. 7; sharp (Bragg) peaks indicating that the NPs were crystalline in nature,[38] which is considered to be superior to amorphous.[39]

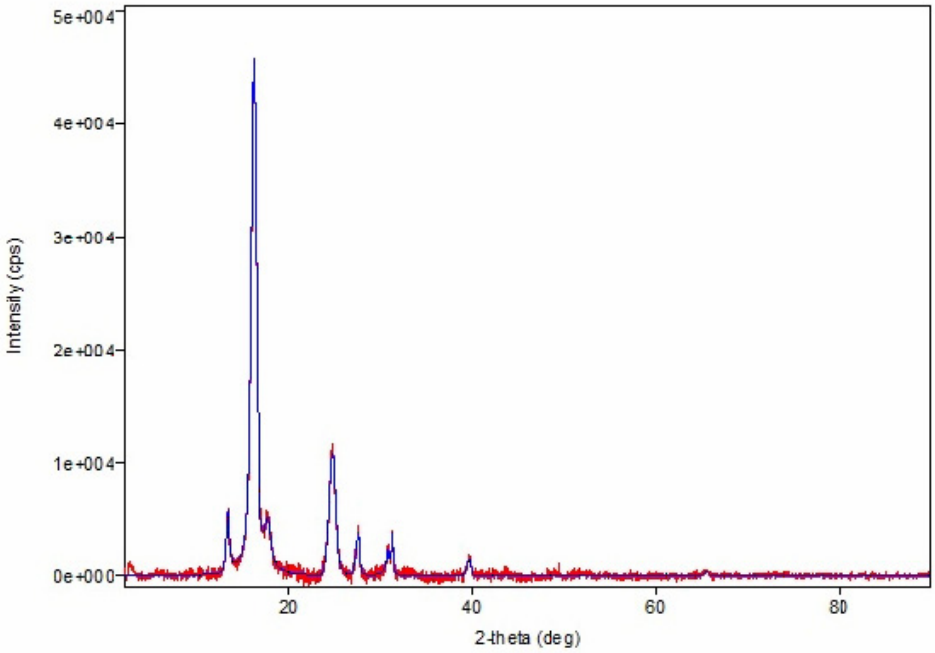

Figure 7. X-ray diffraction pattern of the selenium nanoparticles.

[38] Devanadhan, R., Balaji, G.L. & Lakshmipathy, R. Watermelon rind extract mediated green synthesis of ZnO nanoparticles and its dual application characteristics. *J. Critical Rev.* **7** (2020) 2394–5125.
[39] Phadnis, N.V., Cavatur, R.K. & Suryanarayan R. Identification of drugs in pharmaceutical dosage forms by X-ray powder diffractometry. *J. Pharm. Biomed. Anal.* **15** (1997) 929–943.

3.6 TEM

TEM images revealed that spheroidal nanoparticles were formed. Diameters were in the range 2–100 nm, with an average of around 15–30 nm (Fig. 8).[30]

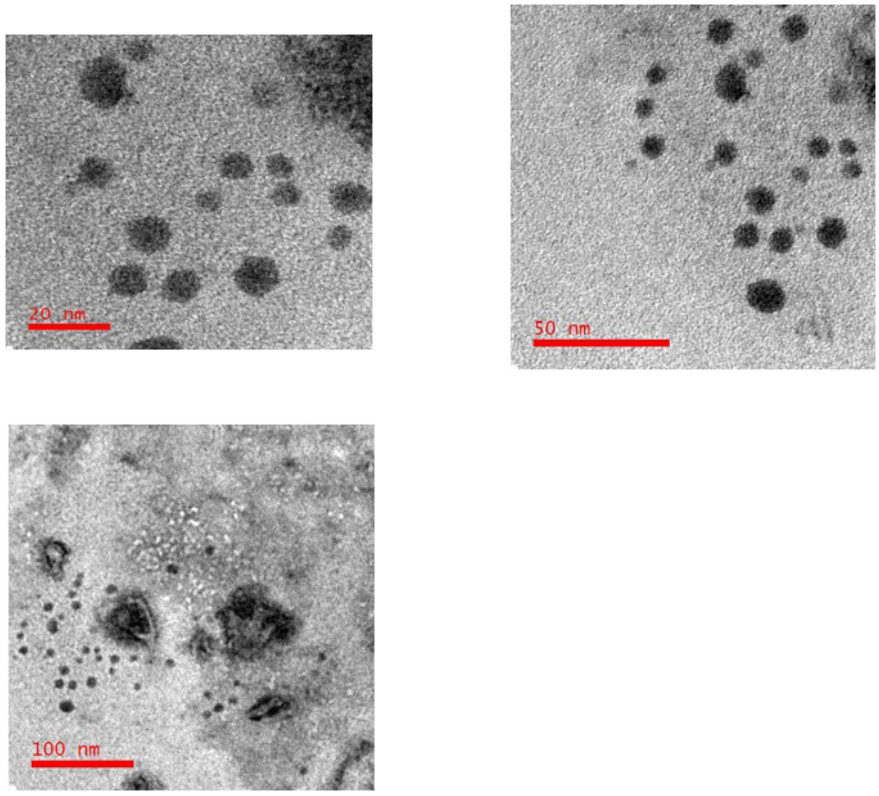

Figure 8. Representative transmission electron microscopy images of selenium nanoparticles.

3.7 PSA & DSC

Laser diffraction revealed that the particle diameters were grouped in two ranges, almost 90% of particles in the 50–200 nm range and the rest in the 48–100 μm range (Fig. 9).[37,40]

The differential scanning calorimetry gave multiple peaks; there was an exothermic transition at about 100 °C and at about 350 °C an endothermic melting peak (Fig. 10).[37,41]

[40] Bell, N.C., Minelli, C., & Shard, A.G. Quantitation of IgG protein adsorption to gold nanoparticles using particle size measurement. *Analyt. Methods* **5** (2013) 4591–4601.

[41] Rolim, P.M., Fidelis, G.P., Padilha, C.E.A., Santos, E.S., Rocha, H.A.O. & Macedo, G.R. Phenolic profile and antioxidant activity from peels and seeds of melon (*Cucumismelo* L. var. *reticulatus*) and their antiproliferative effect in cancer cells. *Braz. J. Med. Biol. Res.* **51** (2018) 1414–1431.

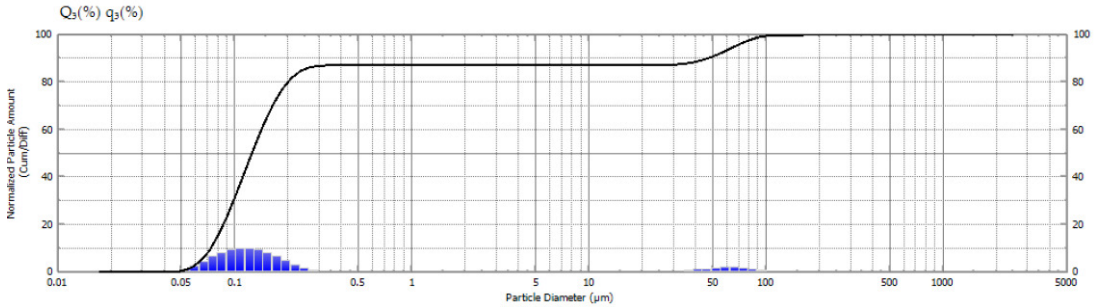

Figure 9. Size analysis by laser diffraction of the selenium nanoparticles.

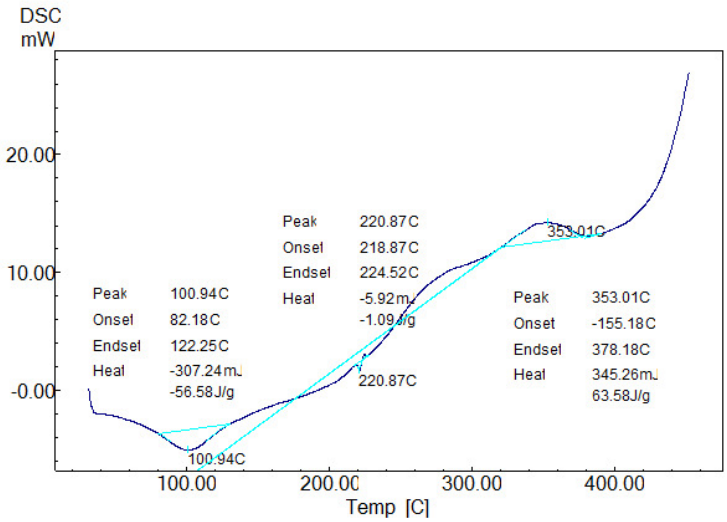

Figure 10. Differential scanning calorimetry of the selenium nanoparticles.

3.8 *In vitro* evaluation of therapeutic effectiveness of watermelon rind against acrylamide-induced cytotoxicity

Cytotoxicity of acrylamide was measured on isolated lymphocytes. Therapeutic effectiveness of aqueous extract of watermelon rind was evaluated after acrylamide exposure. The control (unexposed) group manifested 98% cell viability while the acrylamide (5 mM)-exposed group had only 24% viability. Treatment with aqueous extract of watermelon rind on acrylamide-exposed group showed significant protective activity in a concentration-dependent manner. The dose of 500 µg/mL showed maximum cell viability (Fig. 11). Replotting the data (Fig. 12) showed that the dose-dependence might not be linear. IC_{50} was estimated as 65.30 µg/mL.

We note that rind aqueous extracts exhibit iron- and copper-ion chelating activity. Cell proliferation was inhibited by 20–85% by extracts at 0.1–1.0 mg/mL in renal carcinoma, cervical adenocarcinoma and carcinoma.[42]

[42] Clas, S.D., Dalton, C.R. & Hancock, B.C. Differential scanning calorimetry: applications in drug development. *Pharm. Sci. Technol. Today* **2** (1999) 311–320.

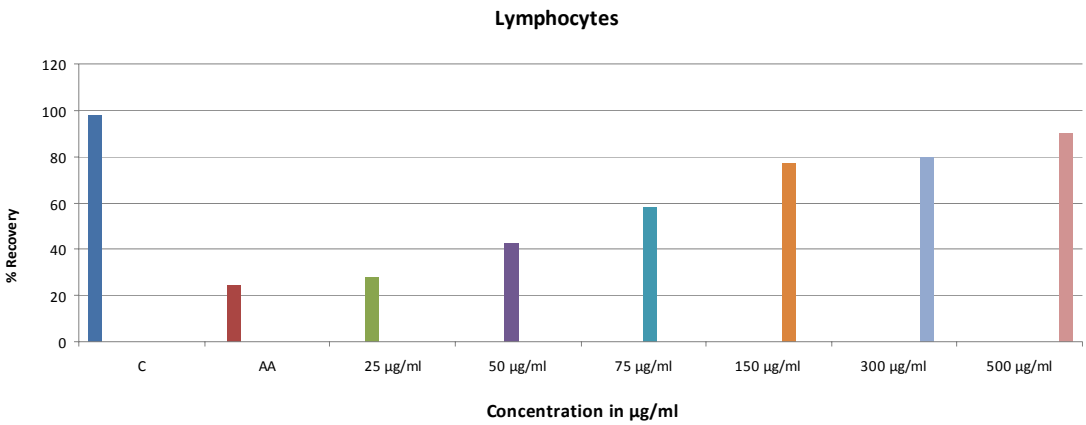

Figure 11. Effect of aqueous extract of watermelon rind at different concentrations on acrylamide (AA)-exposed lymphocytes. C, control with neither AA nor extract; AA, no extract.

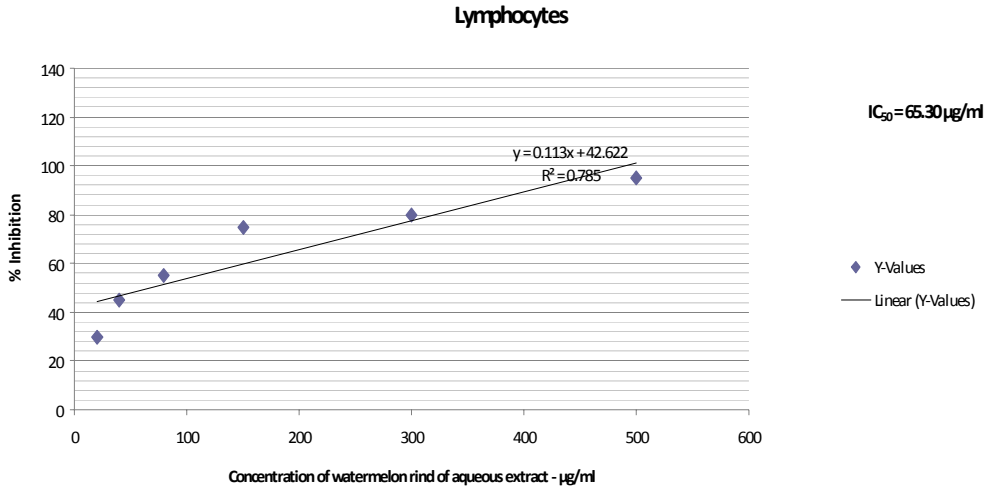

Figure 12. Data of Fig. 11 replotted to determine IC_{50} of aqueous extract of watermelon rind.

4. Summary and conclusions

The present studies show that biosynthesis of Se NPs using watermelon (*Citrullus lanatus)* rind extracts is feasible. Selenium nanoparticles were prepared by a mild chemical reduction method. Characterization by UV–visible spectroscopy reveals the presence of the nanoparticles. FTIR analysis confirms the presence of different functional groups belonging to biomolecules capping the surface of the Se NPs.

Their structural properties were investigated by XRD analysis. The average crystallite size of Se nanoparticles was calculated from the X-ray diffraction (XRD) patterns and found to be 22 nm. TEM revealed typical particle sizes in the range 30–50 nm, in good agreement with PSA (the latter expected to be larger because the hydrodynamic radius is being measured). Excellent

inhibition of acrylamide-induced cell toxicity was observed. These NPs are therefore likely to be therapeutically useful. Furthermore, as "potable selenium" prepared using a nontoxic, natural reducing agent the NPs should be useful as a dietary supplement for combating selenium deficiency.

Acknowledgments

The authors would like to acknowledge the support of the staff of the Dr A.P.J. Abdul Kalam Central Instrumentation Facility at Jiwaji University and, similarly, of the staff running the instrumental facilities at ITM University.